Queen Mary
University of London

Lesional-targeting of neuroprotection to the inflammatory penumbra in experimental multiple sclerosis.

Al-Izki, S; Pryce, G; Hankey, DJ; Lidster, K; von Kutzleben, SM; Browne, L; Clutterbuck, L; Posada, C; Edith Chan, AW; Amor, S; Perkins, V; Gerritsen, WH; Ummenthum, K; Peferoen-Baert, R; van der Valk, P; Montoya, A; Joel, SP; Garthwaite, J; Giovannoni, G; Selwood, DL; Baker, D

For additional information about this publication click this link.
http://qmro.qmul.ac.uk/xmlui/handle/123456789/9650

BRAIN
A JOURNAL OF NEUROLOGY

Lesional-targeting of neuroprotection to the inflammatory penumbra in experimental multiple sclerosis

Sarah Al-Izki,[1] Gareth Pryce,[1] Deborah J.R. Hankey,[2] Katie Lidster,[1] Stephanie M. von Kutzleben,[1] Lorcan Browne,[3] Lisa Clutterbuck,[3] Cristina Posada,[3] A.W. Edith Chan,[3] Sandra Amor,[1,4] Victoria Perkins,[1] Wouter H. Gerritsen,[4] Kim Ummenthum,[4] Regina Peferoen-Baert,[4] Paul van der Valk,[4] Alexander Montoya,[5] Simon P. Joel,[5] John Garthwaite,[3] Gavin Giovannoni,[1] David L. Selwood[3],* and David Baker[1],*

1 Neuroimmunology Unit, Blizard Institute, Barts and the London School of Medicine and Dentistry, Queen Mary University of London, London, UK
2 Neuroinflammation Department, Institute of Neurology, University College London, UK
3 Biological and Medicinal Chemistry, Wolfson Institute for Biomedical Research, University College London, UK
4 Pathology Department, Free University (VU) Medical Centre, Amsterdam, The Netherlands
5 Barts Cancer Institute, Barts and the London School of Medicine and Dentistry, Queen Mary University of London, UK

*These authors contributed equally to this work.

Correspondence to: Dr. Sarah Al-Izki,
Neuroimmunology Unit,
Blizard Institute,
Barts and the London School of Medicine and Dentistry,
Queen Mary University of London,
4 Newark Street,
London E1 2AT, UK
E-mail: s.al-izki@qmul.ac.uk

Progressive multiple sclerosis is associated with metabolic failure of the axon and excitotoxicity that leads to chronic neuro-degeneration. Global sodium-channel blockade causes side effects that can limit its use for neuroprotection in multiple sclerosis. Through selective targeting of drugs to lesions we aimed to improve the potential therapeutic window for treatment. This was assessed in the relapsing-progressive experimental autoimmune encephalomyelitis ABH mouse model of multiple sclerosis using conventional sodium channel blockers and a novel central nervous system-excluded sodium channel blocker (CFM6104) that was synthesized with properties that selectively target the inflammatory penumbra in experimental autoimmune encephalomy-elitis lesions. Carbamazepine and oxcarbazepine were not immunosuppressive in lymphocyte-driven autoimmunity, but slowed the accumulation of disability in experimental autoimmune encephalomyelitis when administered during periods of the inflammatory penumbra after active lesion formation, and was shown to limit the development of neurodegeneration during optic neuritis in myelin-specific T cell receptor transgenic mice. CFM6104 was shown to be a state-selective, sodium channel blocker and a fluorescent p-glycoprotein substrate that was traceable. This compound was >90% excluded from the central nervous system in normal mice, but entered the central nervous system during the inflammatory phase in experimental autoimmune encephalomyelitis mice. This occurs after the focal and selective downregulation of endothelial p-glycoprotein at the blood–brain barrier that occurs in both experimental autoimmune encephalomyelitis and multiple sclerosis lesions. CFM6104 significantly slowed down the accumulation of disability and nerve loss in experimental autoimmune encephalomyelitis.

Therapeutic-targeting of drugs to lesions may reduce the potential side effect profile of neuroprotective agents that can influence neurotransmission. This class of agents inhibit microglial activity and neural sodium loading, which are both thought to contribute to progressive neurodegeneration in multiple sclerosis and possibly other neurodegenerative diseases.

Keywords: multiple sclerosis; animal models; experimental allergic encephalomyelitis; neural repair

Abbreviation: EAE = experimental autoimmune encephalomyelitis

Introduction

Multiple sclerosis is the major cause of non-traumatic disability in young adults (Compston and Coles, 2008). It is clear that relapsing multiple sclerosis can be controlled by the action of peripherally-active immunosuppressive agents that reduce CNS atrophy (Gunnarsson *et al.*, 2011; Marta and Giovannoni, 2012). These serve to limit waves of inflammatory cells entering the CNS from the blood that are manifest in relapsing disease in humans and in experimental autoimmune encephalomyelitis (EAE) animal models of multiple sclerosis (Allen *et al.*, 1993; Lassmann, 2013). These cause focal lesions that are characterized by demyelination and variable degrees of axonal loss, gliosis and microglial activation. The microenvironment in lesions is believed to progressively damage axons and make them susceptible to chronic degeneration (Pryce *et al.*, 2005; Hampton *et al.*, 2008), which underpins the accumulation of chronic disability (Lassmann, 2013). This secondary progression appears to be unresponsive to peripheral immunosuppression in both multiple sclerosis and EAE and is currently untreatable (Coles *et al.*, 1999; Pryce *et al.*, 2005; Dutta and Trapp, 2011; Al-Izki *et al.*, 2012).

Although, the precise mechanisms of axonal pathology are unproven, axonal pathology in acute multiple sclerosis lesions is associated with macrophage and glial cell activation, excitotoxicity and loss of metabolic support (Dutta and Trapp, 2011; Lee *et al.*, 2012; Parpura and Verkhratsky, 2012). Demyelination also leads to neuronal sodium and calcium channel upregulation and increased energy demands that leave demyelinated axons vulnerable to further damage (Craner *et al.*, 2004). Voltage-gated sodium channels (Na_v) are redistributed from the nodes of Ranvier along demyelinated axonal segments to maintain neural conduction (Craner *et al.*, 2004). This facilitates sodium loading that is compounded by loss of activity of energy-dependent sodium pumps following mitochondrial dysfunction secondary to a complex inflammatory cascade (Dutta and Trapp, 2011). This can lead to the formation of toxic levels of axoplasmic calcium (Kapoor *et al.*, 2003; Dutta and Trapp, 2011), which trigger further neuroaxonal damage. This, in conjunction with and altered astrocytic control of neurotransmitter balance, leads to progressive disability that no longer responds to systemic immunosuppression (Dutta and Trapp, 2011; Lee *et al.*, 2012; Parpura and Verkhratsky, 2012). Although these mechanisms highlight potential therapeutic targets (Fern *et al.*, 1993; Waxman, 2008), many of them are involved in normal nerve function; inhibiting their function may therefore be associated with side effects that can limit their clinical use (Kapoor *et al.*, 2010; Gnanapavan *et al.*, 2013). This is particularly a problem in progressive multiple sclerosis where accumulating nerve loss reduces compensatory or reserve capacity and lowers the threshold for side effects from drugs that alter neurotransmitter function. There is an urgent, unmet need to find new treatments for progressive multiple sclerosis.

Studies in myelin oligodendrocyte glycoprotein (MOG) peptide-induced EAE in C57BL/6 and Biozzi ABH mice have shown that Na_v blockers can ameliorate the development of neurological disease (Lo *et al.*, 2003; Black *et al.*, 2006, 2007). In many instances the treatment benefit of Na_v blockers could be attributed to immunosuppression that prevented lesion formation and the development of disease (Craner *et al.*, 2005; Black *et al.*, 2007). However, in Biozzi ABH mice, the myelin peptide used to induce disease to examine the influence of carbamazepine (Black *et al.*, 2007) was subdominant even within the MOG protein, which in itself is not the major encephalitogenic auto-antigen (Amor *et al.*, 1994; Pryce *et al.*, 2005; Smith *et al.*, 2005). After active sensitization with spinal cord homogenate in Freund's adjuvant the initial paralytic attack is inflammatory, but is not associated with significant demyelination and neuroaxonal loss. The latter occurs following the development of spontaneous or induced-relapsing disease (Baker *et al.*, 1990; Hampton *et al.*, 2008; Jackson *et al.*, 2009; Al-Izki *et al.*, 2012). This stage of disease in the ABH model allows one to discriminate between the effects of therapies that target both immunosuppression and/or neuroprotective mechanisms. Neuroprotection is seen by the slower accumulation of residual neurological deficits and slower loss of motor control on RotaRod activity, which have a good correlation with spinal nerve content (Al-Izki *et al.*, 2012).

As demyelinated lesions centre around the vasculature (Baker *et al.*, 1990; Lassmann, 2013), we hypothesized that it would be possible to use blood–brain barrier activities, notably exploiting the actions of energy-dependent, adenosine triphosphatase binding cassette (ABC) transporters, such as p-glycoprotein (Miller *et al.*, 2008), to selectively target potentially neuroprotective agents to multiple sclerosis lesions. We show this activity using a novel CNS-excluded Na_v blocker, which is a p-glycoprotein substrate, and was targeted to lesions after the selective loss of p-glycoprotein that occurs in both multiple sclerosis and EAE lesions.

Materials and methods

Multiple sclerosis tissue

Brain tissue samples were obtained from the Netherlands Brain Bank. The Netherlands Brain Bank received permission to perform autopsies

for the use of tissue and for access to medical records for research purposes from the Ethical Committee of the VU University Medical Centre, Amsterdam, The Netherlands. A total of 10 paraffin-embedded tissue blocks from patients with multiple sclerosis, containing active, chronic active and chronic inactive lesions, and one white matter block from six different donors without neurological disease were selected. Normal-appearing white matter and lesions in white matter were selected on the basis of post-mortem MRI. All patients with multiple sclerosis and control subjects, or their next of kin, had given informed consent for autopsy and use of their brain tissue for research purposes. Analysis of tissue was supported by ethical review panels within The Netherlands and UK (REC 08/H0722/26).

Animals

Adult female (6–8 weeks), pathogen-free, Biozzi ABH mice and C57BL/10.RIII mice were purchased from Harlan UK Ltd, or male and female ABH mice were bred at Queen Mary University of London. C57BL6.Cg-Tg (Thy1-CFP)23Jrs.Tg (Tcra2D2, Tcrb2D2)1Kuch/J transgenic mice, which express a neuronally-restricted, Thy1-promoter driven expression of cyan fluorescent protein (CFP) that is limited to retinal ganglion cells within the retina (Feng et al., 2000) and a H-2b-restricted MOG-specific T cell receptor (Bettelli et al., 2003; Guan et al., 2006), were from stock bred at Queen Mary University of London (Lidster et al., 2013). Methods of housing, allocation to groups and other reporting elements including blinding, relevant to the ARRIVE guidelines have been reported previously (Al-Izki et al., 2012). All procedures were approved by the local ethical review processes and were performed in accordance with the UK Animal (Scientific Procedures) Act 1986.

Chemicals

Carbamazepine, oxcarbazepine, memantine hydrochloride and minocycline hydrochloride were purchased from Sigma Aldrich. CFM6104 [N-((5-(2-(2-(1h-imidazol-1-yl)ethyl)-2h-indazol-3-yl)-1,2,4-oxadiazol-3-yl)methyl)-3-methylbenzamide] is a novel, non-selective, state-dependent sodium channel blocker. The synthesis will be described elsewhere (Browne et al., submitted for publication). This has no detectable activity on active receptor subtypes ($IC_{50} > 30\,\mu M$), but had modest activity ($IC_{50} = \sim 20$–$25\,\mu M$) on inactive $Na_v1.1$, $Na_v1.2$, $Na_v1.5$, $Na_v1.6$, $Na_v1.7$ receptors (Browne et al., submitted for publication). CFM6104 was dissolved in a 1:1 solution of dimethyl sulphoxide and PBS and allowed to cool before administration intraperitoneally, or dissolved in ethanol:cremophor:PBS 1:1:18. Minocycline hydrochloride was adjusted to pH 7, using 10 N sodium hydroxide before use. These were administered either daily just before or after the anticipated onset of relapsing disease.

In vivo T cell proliferation assays

The contact sensitizer 4-ethoxymethylene-2-phenyl-2-oxazolin-5-one (oxazolone, OX, Sigma) was dissolved (25 mg/ml) in 4:1 acetone:olive oil. Mice (n = 3 per group) received epicutaneous application of either 25 µl of 2.5% oxazolone or acetone:olive oil on the dorsum of the ear on Day 0 (O'Neill et al., 1992). The draining auricular lymph nodes were removed 3 days later and the induced proliferative response was assessed as previously described. Briefly, 5×10^5 cells per well were cultured in RPMI-1640 medium with glutamate (Gibco®, Invitrogen), supplemented with 0.5 mM sodium, in round-bottomed 96-well plates overnight at 37°C in a humidified atmosphere of 5% CO_2. T cell proliferation was assessed using the CellTiter 96® AQueous

Non-Radioactive Cell Proliferation Assay according to the manufacturer's instructions (Promega) and the absorbance was recorded at 490 nm. Animals received daily intraperitoneal injections of either vehicle or CFM6104 from Day 0–3.

Induction of relapsing-progressive experimental autoimmune encephalomyelitis

Mice were injected subcutaneously with 1 mg freeze-dried mouse spinal cord homogenate in Freund's adjuvant on Days 0 and 7 as described previously (Al-Izki et al., 2012). After the initial paralytic disease and subsequent remission, a relapse was induced by a further injection of spinal cord homogenate in Freund's adjuvant on Day 28 to induce a relapse 7 days later (Al-Izki et al., 2012). Studies were randomized, blinded and powered as described previously (Al-Izki et al., 2012). Neurological scores were graded as: 0 = normal; 1 = limp tail; 2 = impaired righting reflex; 3 = hindlimb paresis; 4 = complete hind-limb paralysis; and 5 = moribund/death (Al-Izki et al., 2012). Motor control and co-ordination was assessed on an accelerating (4–40 rpm, accelerating at 6 rpm/25 s) RotaRod (ENV-575 M, Med Associates Inc.) as described previously (Al-Izki et al., 2012). This was performed 1 day before induction of relapse and 1 day before termination of the experiment on Day 49–50. RotaRod assessment was performed blinded to treatment. Animals were randomized to vehicle or treatment based on their RotaRod scores.

At the end of the experiment the spinal cord was removed and an ELISA for heavy chain neurofilament on spinal cord was performed and total nerve content of each spinal cord was estimated following calibration against neurofilament protein standards as described previously (Jackson et al., 2005).

Induction of experimental autoimmune uveitis

C57BL/10.RIII mice were injected subcutaneously with 25 µg interphotoreceptor binding peptide residues 161–182 in Freund's adjuvant on Days 0 and 7 as described previously (Hankey et al., 2001). On Day 21 post-induction animals were killed and eyes were removed, fixed, wax embedded and 5 µm sections through the optic nerve head were stained with haematoxylin and eosin. Sections were scored blinded to treatment on a 0–6 scale to assess the degree of cellular infiltration and a 0–5 scale to assess retinal nerve damage as described previously (Hankey et al., 2001).

Induction of optic neuritis mouse model

Optic neuritis was induced in C57BL/6-.Cg-Tg (Thy1-CFP)23Jrs.Tg (Tcra2D2, Tcrb2D2)1Kuch/J transgenic mice after administration of 150 ng Bordetella pertussis toxin (Sigma Aldrich) in PBS on Days 0 and 2 (Bettelli et al., 2003; Lidster et al., 2013) Subclinical EAE and optic neuritis within the optic nerve was augmented following the injection of 250 µg Z12 rat IgG2b mouse myelin oligodendrocyte-specific demyelinating antibody (Piddlesden et al., 1993; Lidster et al., 2013) on Day 14. Animals were injected daily on Days 0–21 with the compounds. Animals were killed on Day 21 post-induction and eyes were enucleated and immersed in 4% paraformaldehyde (Sigma Aldrich) in PBS pH 7.4 overnight. The retinas were dissected and the cornea, sclera, lens, hyaloid vasculature and connective tissue were removed in $2\times$ normal strength PBS. Four radial incisions were

cut around the retinas and flat mounts were mounted onto slides and cover-slipped with anti-fade glycerol (CitiFluor Ltd). The retinal flat mounts were imaged by fluorescent microscopy and retinal ganglion cells density was calculated by counting CFP expressing retinal ganglion cells using stereology software with a fractionator probe and the number cells in the four quadrants around the optic nerve head counted (Lidster *et al.*, 2013). The results are expressed as mean $\pm$ standard error of the mean (SEM).

Liquid chromatography–mass spectroscopy

Pharmacokinetic studies on plasma and brain samples using liquid chromatography-mass spectroscopy (LC-MS/MS) with a sensitivity of 3 ng/ml, was performed by Merck Serono. In addition plasma and spinal cords were harvested from ABH mice 30 min after the intraperitoneal injection of 10 mg/kg CFM6104 in ethanol:cremophor:PBS 1:1:18. Spinal cords were homogenized in 2 ml eppendorf tubes using a 5 mm steel bead and TissueLyzer-II (Qiagen) set at 25 Hz for 5 min. Twenty microlitres of the homogenate or plasma was extracted by 100 µl acetonitrile (with internal standard, coumaphos). Samples were then incubated on ice for 30 min, centrifuged and the supernatant was analysed using UPLC-MS/MS. Analytes were resolved using an Accela UPLC (Thermo Scientific) equipped with 1.7 µm PFP Kinetex 2.1 × 50 mm UPLC column (Phenomenex) and a mobile phase gradient of buffer A (water + 0.1% formic acid) and buffer B (acetonitrile + 0.1 formic acid) at a flow rate of 500 µl/min. Eluting compounds of interest were detected using a TSQ Vantage mass spectrometry system (Thermo Scientific). The optimum transitional daughter ions mass of each analyst were as follows: CFM6104 m/z 414.1 → 239.1 and coumaphos m/z 363.3 → 227. The sensitivity was 1 ng/ml.

P-glycoprotein assay

Assessment of vascular permeability was performed using the Pgp-Glo^{TM} assay (Promega) containing recombinant human ABCB1 in membranes according to the manufacturer's instructions. Briefly, samples were preincubated with ATP before incubation with 100 µM compound or positive control. The residual ATP was assayed by luciferin bioluminescence. In addition, monolayer permeability and efflux was assessed in a bi-directional transport assay by Merck Serono using CacoReady^{TM} (ReadyCell SL). Briefly, differentiated and polarized Caco-2 cell barriers were grown on polycarbone microporous filters in a 24-well format. One micrometre compounds were incubated for 120 min pH 7.4/7.4 apical/basolateral after apical or basolateral application and basolateral or apical sampling, respectively, in the presence or absence of 1 µM cyclosporin A, which is a p-glycoprotein inhibitor. Drug concentrations were assessed by LC-MS/MS using an API 5500-Trap.

Immunohistochemistry

Formalin-fixed paraffin-embedded mouse and human tissue was sectioned at 5 µm. Human tissue was stained for proteolipid protein (PLP, clone plpc1, Serotec Ltd), HLA-DR (clone LN3, Dako), p-glycoprotein/CD243 (clone C219, Abcam), breast cancer resistance protein (BCRP/CD338, clone 6D170, US Biological) and the endothelial marker glucose transporter-1 (Glut-1; a kind gift from Jack van Horssen, VUMC). Sections were deparaffinized in xylene and rehydrated through graded alcohol into distilled water. Endogenous peroxidase activity was

quenched using 0.3% hydrogen peroxide in methanol. For HLA-DR, p-glycoprotein, BCRP (now known as ABCG2) and Glut-1 detection, slides were rinsed with distilled water and transferred to citric acid for heat-induced antigen retrieval. After microwave irradiation for 5 min on the high setting and for 10 min on the medium setting, slides were cooled to room temperature and rinsed in PBS. Serial sections were incubated overnight with either anti-HLA-DR (1:100), proteolipid protein (1:500), p-glycoprotein (clone C219, 1:50); BCRP (1:400); Glut-1 (1:1000). Slides were incubated with Envision Kit horseradish peroxidase-labelled anti-mouse/rabbit Ig (Dako) for 30 min at room temperature, and finally diaminobenzidine tetrachloride. Between incubation steps, sections were thoroughly washed with PBS. After a short rinse in tap water sections were incubated with haematoxylin for 1 min and extensively washed with tap water for 10 min. Finally, sections were dehydrated with ethanol followed by xylol and mounted with Entellan (Merck). All antibodies were diluted in PBS containing 0.1% bovine serum albumin (Boehringer-Mannheim), which also served as a negative control. Immunofluorescence was carried out on sections from three patients with multiple sclerosis to depict Glut-1, p-glycoprotein and cell nuclei with DAPI. After antigen retrieval and blocking for 1 h with 5% normal goat serum, the sections were incubated with p-glycoprotein (1:20) and Glut-1 (1:50) overnight at room temperature. The sections were then rinsed in PBS and the secondary antibodies (goat anti-rabbit Ig Alexa Fluor® 488 and goat anti-mouse Ig Alexa Fluor® 594) applied for 1 h. After washing in PBS, sections where incubated with 0.5% Sudan Black (Sigma) and nuclei visualized with DAPI, washed and mounted in glycerol/PBS. This protocol was also used on formalin fixed-snap-frozen mouse tissues from chronic secondary progressive EAE tissues with the exception of a mouse-on-mouse blocking step using CleanVision (Immunologic).

Statistical analysis

The neurological scores are presented as the mean daily neurological score $\pm$ SEM. Differences in scores in EAE and experimental autoimmune uveitis were assessed using Mann-Whitney U statistics. The parametric data, including RotaRod and retinal ganglion cells number, were assessed using a student's *t*-test or one-way ANOVA incorporating tests for equality of variance using Sigmastat/Sigmaplot software (Systat Software, Inc.).

Results

Na$_v$ blockade is neuroprotective in central nervous system autoimmunity

Spinal cord homogenate-induced relapsing-progressive disease in Biozzi ABH mice was used to examine the neuroprotective influence of Na$_v$ blockage. When drug administration was avoided during the sensitization periods, there was no evidence of any marked immunosuppressive effect of administration intraperitoneally of either 1 mg/kg or 10 mg/kg carbamazepine. All animals developed EAE with comparable high severity (Fig. 1A). This indicated marked inflammatory cell recruitment into the CNS (Allen *et al.*, 1993; Jackson *et al.*, 2009), in contrast to that occurring with T cell immunosuppressive agents (Watson *et al.*, 1991; Baker *et al.*, 1992; O'Neill *et al.*, 1992, 1993). The maximum disease score of animals in relapse was comparable between vehicle and carbamazepine-treated animals (Fig. 1A and B); however, the
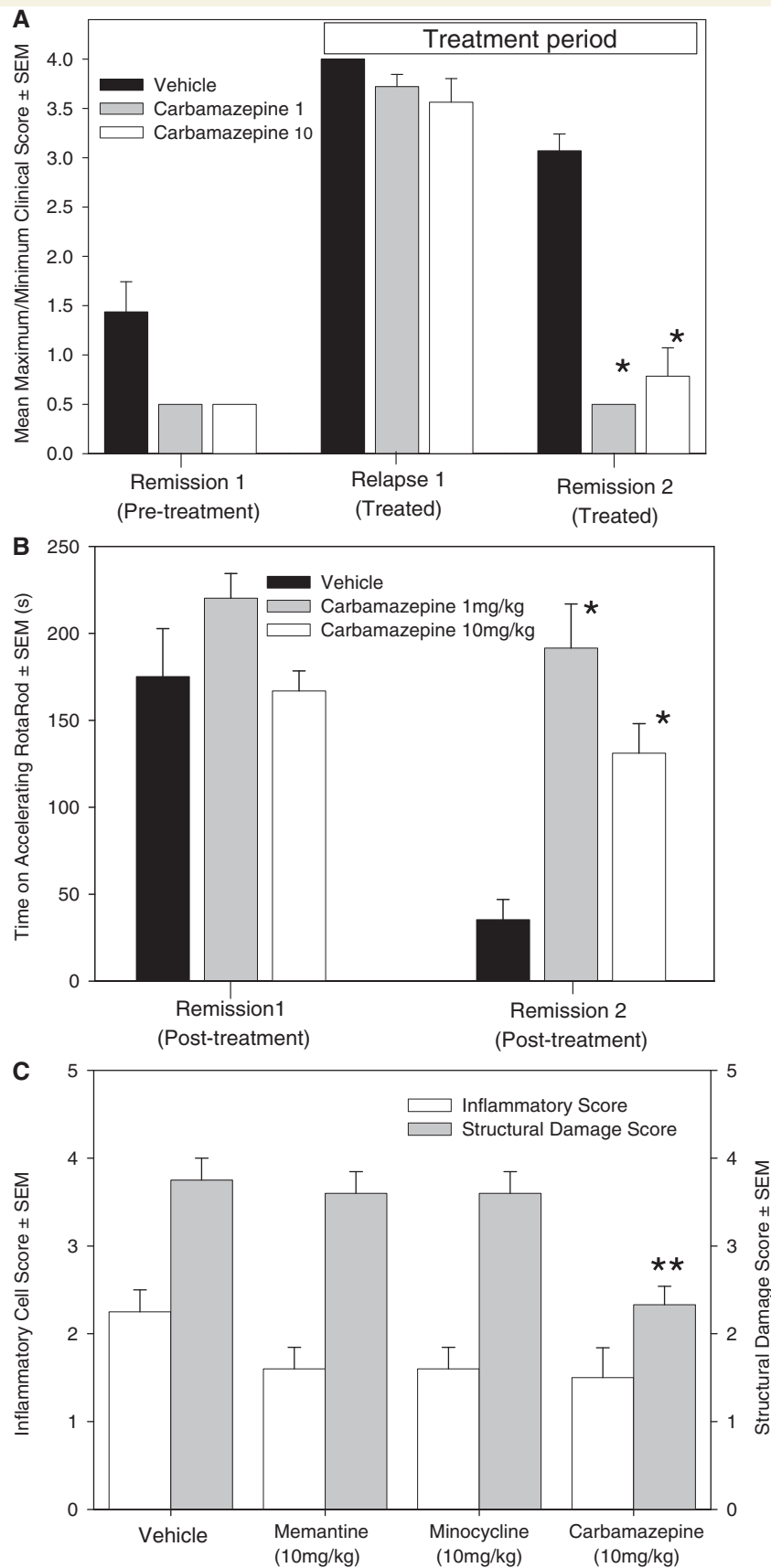
Figure 1 Low-dose carbamazepine inhibits the accumulation of neurological deficit during CNS autoimmunity. (**A** and **B**) ABH mice were injected with mouse spinal cord homogenate in Freund's adjuvant on Days 0 and 7 post-induction (p.i.) to induce EAE and on Day 27

residual deficit during remission from relapse was significantly reduced ($P < 0.001$). Vehicle-treated mice remitted to a score of 3.1 ± 0.2 compared with 0.8 ± 0.1 (1 mg/kg) or 0.8 ± 0.3 (10 mg/kg) for carbamazepine-treated animals. Although there was no statistically significant difference in the scores of groups before treatment onset it appeared that following randomization to the RotaRod score, there were more animals with residual limb paresis in the vehicle group after unblinding (Fig. 1A). As a consequence of this, for subsequent experiments we set an exclusion criterion such that animals with residual limb paresis after the initial attack were not entered into the randomization or treatment processes. Applying this criterion to remove animals from the experiment (Fig. 1A) such that the score before treatment onset was 0.5 ± 0.0, the data, however, still demonstrated that there was no difference in the severity of the relapse [3.6 ± 0.4 (vehicle) verses 3.6 ± 0.2 (10 mg/kg) and 3.7 ± 0.1 (1 mg/kg) carbamazepine] but carbamazepine-treated animals demonstrated a significantly better recovery [2.6 ± 0.7 (vehicle) verses 0.8 ± 0.3 (10 mg/kg) and 0.5 ± 0.0 (1 mg/kg) carbamazepine ($P < 0.05$)]. This recovery was mirrored in the motor functional analysis using the RotaRod whereby animals treated with carbamazepine were able to stay on the RotaRod significantly ($P < 0.001$) longer (1 mg/kg 191.6 ± 25.3 s, 10 mg/kg 131 ± 17.1 s) than those treated with vehicle (35.4 ± 11.6 s) after 14 days of treatment.

These data suggest that treatment does not stop the cause of disease or lesion formation indicating a lack of lymphoid cell-induced immunosuppression (Baker *et al.*, 2011). In an additional model (Fig. 1C), experimental autoimmune uveitis in C57BL/10.RIII mice (Hankey *et al.*, 2001), daily intraperitoneal injection from Day 8–22 of 10 mg/kg carbamazepine limited the accumulation of retinal nerve damage in the eye ($P < 0.02$), without significantly influencing the degree of immune infiltration with the retina (Fig. 1C). This was more neuroprotective than similar delivery of 10 mg/kg memantine (a weak *N*-methyl-D-aspartate glutamate receptor antagonist) or minocycline (microglial-inactivating antibiotic).

Time window for Na$_v$ blockers to influence the inflammatory penumbra

While treatment was therapeutic as animals were already sensitized and disease had manifested before therapy was initiated

(Fig. 1A and B), the protective effect of administration after disease onset was investigated (Fig. 2). Carbamazepine and oxcarbazepine were administered at various times after the onset of signs and the influence on recovery assessed. In the first set of experiments, treatment with carbamazepine, oxcarbazepine or vehicle was initiated at the onset of signs (Day 0) or 2 days later and continued until the end of the experiment ∼Day 50 post-induction. Animals treated with carbamazepine and oxcarbazepine from Day 0 (day of relapse onset) had significantly less disability ($P < 0.01$ and $P < 0.05$, respectively) than those treated with vehicle control as assessed using the neurological scoring system. This improvement was also seen in the RotaRod, in which animals treated with both sodium channel blockers performed significantly ($P < 0.001$) better than those treated with vehicle control. When treatment was delayed a further 2 days after onset of relapse, the beneficial effect on the neurological score was not as pronounced, but there was some improvement in RotoRod scores (Fig. 2B and D). In an additional experiment, treatment with oxcarbazepine was delayed until Day 4 post disease-onset (Fig. 2E and F). At this time point, 4 days post disease-onset, the drug had no effect on clinical score or RotaRod performance (Fig. 2E and F). Animals to be treated were selected before randomization to treatment on the basis that their weight had stabilized or improved from the previous day. Paralysed animals that are gaining weight are beginning to remit and have a reduction in blood–brain barrier dysfunction manifest as cellular recruitment and plasma protein extravasation (Al-Izki *et al.*, 2012). This suggests that the Na$_v$ blocking compounds were most active during lesion formation and periods of blood–brain barrier dysfunction. Once the natural regulatory mechanisms that limit relapse were initiated, Na$_v$ blockage failed to augment the recovery response.

Although RotoRod activity strongly correlates with spinal nerve loss (Al-Izki *et al.* 2012), unfortunately it was not possible to measure spinal cord nerve content for technical reasons. Therefore, to demonstrate the neuroprotective effects of these compounds histologically, additional experiments were performed using a transgenic mouse model of multiple sclerosis that develops optic neuritis, where EAE typically remains subclinical after stimulation of MOG-specific transgenic T cell receptors (Lidster *et al.* 2013). As a consequence of autoimmunity to MOG within the optic nerve, consequent retinal ganglion cells loss within the retina can subsequently be

Figure 1 Continued
post-induction to induce a relapse. Animals were injected daily intraperitoneally with either 0.1 ml vehicle (black bar $n = 7$), 1 mg/kg (grey bar $n = 7$) or 10 mg/kg (white bar $n = 7$) carbamazepine from Day 33 onwards. Animals were monitored for the development of clinical disease and the results represent: (**A**) The mean maximal clinical score, during the initial acute attack ∼Days 15–20 and the clinical relapse ∼Days 34–40, or the mean minimal clinical score during remission from paralytic attacks. (**B**) The time taken to fall from an accelerating RotaRod was monitored pretreatment on Day 28 or on Day 48 post-disease induction, when the experiment was terminated. (**C**) B10.RIII mice were injected with interphotoreceptor binding peptide in Freund's adjuvant on Days 0 and 7. Animals were sacrificed on Day 21 and the eyes were fixed, sectioned at the level of the optic nerve head and stained with haematoxylin and eosin. Animals were treated daily intraperitoneally from Day 8–21 with either vehicle ($n = 5$), 10 mg/kg memantine ($n = 5$), 10 mg/kg minocycline ($n = 5$) or 10 mg/kg carbamazepine ($n = 6$). These were scored to assess the degree of ocular infiltration on a 0–6 scale, where typically peak infiltration score of 4–5 occurs ∼Day 10 and were scored for retinal structural damage on a 0–5 scale, which typically reaches a plateau by ∼Day 16 onwards. Results represent the mean ± SEM score. *$P < 0.05$ compared with vehicle-treated animals. **$P < 0.02$ compared with vehicle.
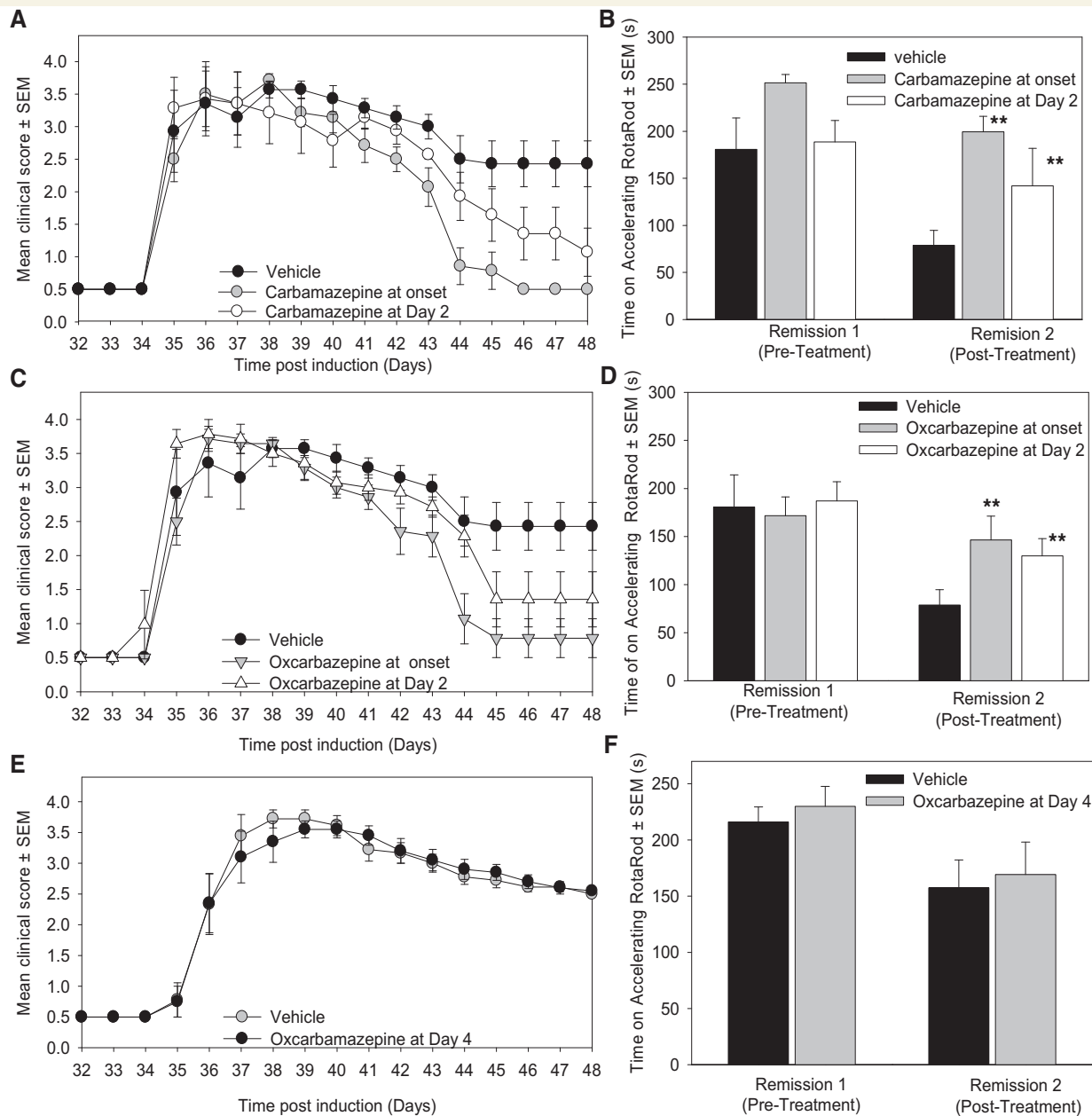
Figure 2 Carbamazepine and oxcarbazepine inhibit the accumulation of neurological deficit days following onset of signs during EAE. ABH mice were injected with 1 mg mouse spinal cord homogenate in Freund's adjuvant on Days 0 and 7 post-induction to induce EAE and this was repeated on Day 27 post-induction to induce a relapse. Animals were injected daily intraperitoneally with either vehicle or 10 mg/ kg carbamazepine or oxcarbazepine at the (**A–D**) onset of signs on Day 35 (onset) or 2 days (Day 2) later, or (**E** and **F**) 4 days (Day 4) after onset of signs of relapse. Animals were monitored for the development of clinical disease and the results represent: (**A**, **C** and **E**) the mean daily clinical score after induction of relapse. (**B**, **D** and **F**) The time taken to fall from an accelerating RotaRod was monitored pretreatment on Day 25 or on Day 48 post-disease induction, when the experiment was terminated. Results represent the mean ± SEM of eight animals per group. *$P < 0.05$, **$P < 0.01$, ***$P < 0.001$ compared with vehicle-treated animals.

monitored using fluorescence microscopy to detect CFP expressing retinal ganglion cells (Fig. 3A–D). Sodium channel blockage with either 10 mg/kg carbamazepine or oxcarbazepine (Fig. 3A, B and D) both significantly ($P < 0.05$) limited the amount of nerve loss compared to the influence of vehicle (ECP) occurring as a consequence of optic neuritis (Fig. 3C and D).

Selective loss of energy-dependent efflux transporters during neuroinflammatory disease

The clinical use of Na$_v$ channel blockers in multiple sclerosis can be associated with the development of neurological side effects at doses below those used for anti-convulsive activity in epilepsy
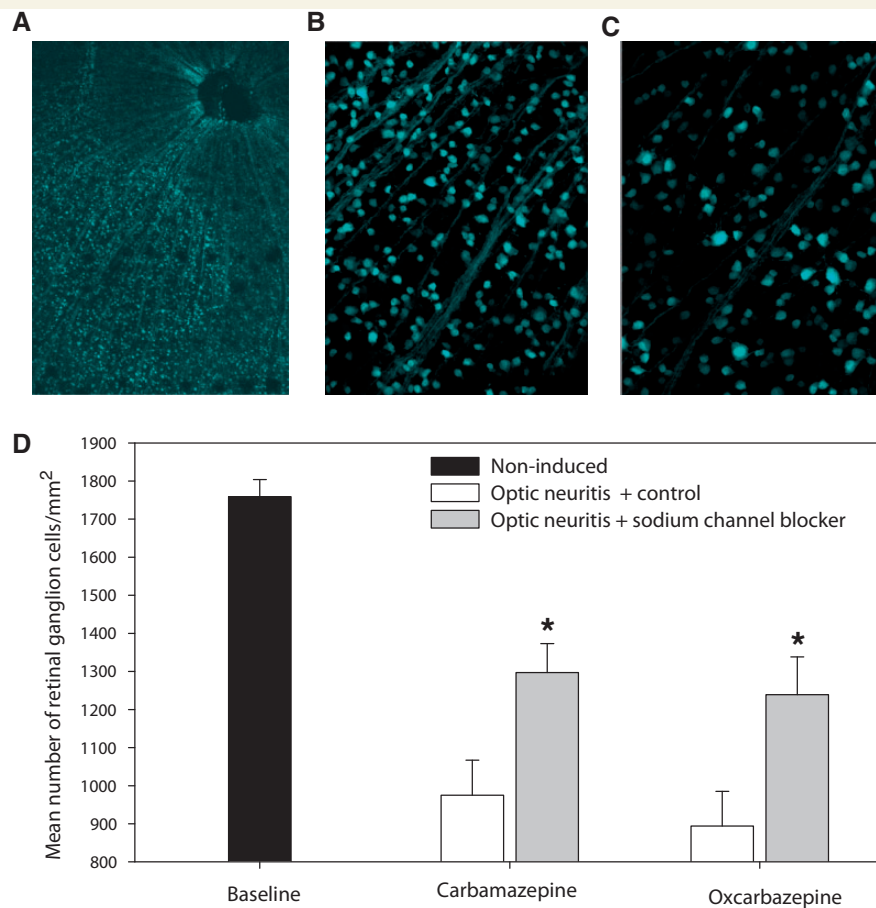
Figure 3 Carbamazepine and oxcarbazepine inhibits the development of neurogeneration. C57BL/6 transgenic mice expressing MOG-specific T cell receptors and retinal ganglion cells-restricted CFP were 150 ng *B. pertussis* toxin on Days 0 and 2 and demyelination was augmented following injection of 250 μg demyelinating antibody on Day 14. Animals were injected intraperitoneally daily with either vehicle or 10 mg/kg carbamazepine or oxcarbazepine in ethanol:cremophore:PBS vehicle from Days 0–21. Animals were sacrificed and the eyes removed on Day 21 and retinal flat mounts were prepared and the number of retinal ganglion cells within the retina were counted. (**A** and **B**) Retinal ganglion cells in oxcarbazepine-treated animals at (**A**) low and (**B**) higher power. (**C**) Retinal ganglion cells in a vehicle-treated animal at high power. (**D**) Retinal ganglion cells number stereologically counted in either normal ($n = 24$) animals or mice induced to develop optic neuritis and treated either with vehicle ($n = 14$) or carbamazepine ($n = 7$) in one experiment or vehicle ($n = 22$) or oxcarbazepine ($n = 13$) in a separate experiment. Results represent the mean ± SEM. *$P < 0.05$, **$P < 0.01$, ***$P < 0.001$ compared with vehicle-treated animals.

(Kapoor *et al.*, 2010). Therefore, by selectively targeting potential neuroprotective drugs to active lesions, it may be possible to improve the therapeutic window for this class of drugs. Although the nature of blood–brain barrier dysfunction is varied, it is well-known that this is associated with leakage of cells and plasma proteins in EAE and multiple sclerosis (Butter *et al.*, 1991; Al-Izki *et al.*, 2012). One aspect that contributes to this—as shown here—is the selective loss of p-glycoprotein (ABCB1) within lesions. This occurs both in EAE (Fig. 4) and multiple sclerosis (Fig. 5) lesions. In comparison with vascular p-glycoprotein expression in normal mice (Fig. 4A), p-glycoprotein was selectively lost in active lesions during relapsing disease (Fig. 4B and C) in comparison with BCRP (now known as ABCG2, Fig. 4D) and compared with non-inflamed tissues (Fig. 4C and E–K). P-glycoprotein was lost from the vasculature (Fig. 4H–K) as shown using double-labelling of p-glycoprotein with Glut-1 on endothelia (Fig. 4L–N).

This vascular loss of p-glycoprotein remained during post-relapsing secondary progressive EAE (Fig. 4L–N) and in comparison with normal brain tissue (Fig. 5A) and normal-appearing white matter in multiple sclerosis (Fig. 5B), p-glycoprotein was also absent from the vasculature in chronic inactive in multiple sclerosis lesions (Fig. 5C and D). Interestingly there was an upregulation of astrocytic p-glycoprotein in such chronic lesions (Fig. 5D) and non-vascular p-glycoprotein expression seemed to occur in EAE lesions (Fig. 4B and L–N). Again, in humans there was selective loss of p-glycoprotein in contrast to vascular expression of BCRP in multiple sclerosis lesions (Fig. 5E). Double-labelling of p-glycoprotein with endothelial Glut-1 (Fig. 5F–K) demonstrated vascular expression of p-glycoprotein in vessels in normal-appearing white matter (Fig. 5F–H), which was reduced or lost in lesions (Fig. 5I–K) although it was detected in non-Glut-1-positive cells even in active multiple sclerosis lesions (Fig. 5J and K).
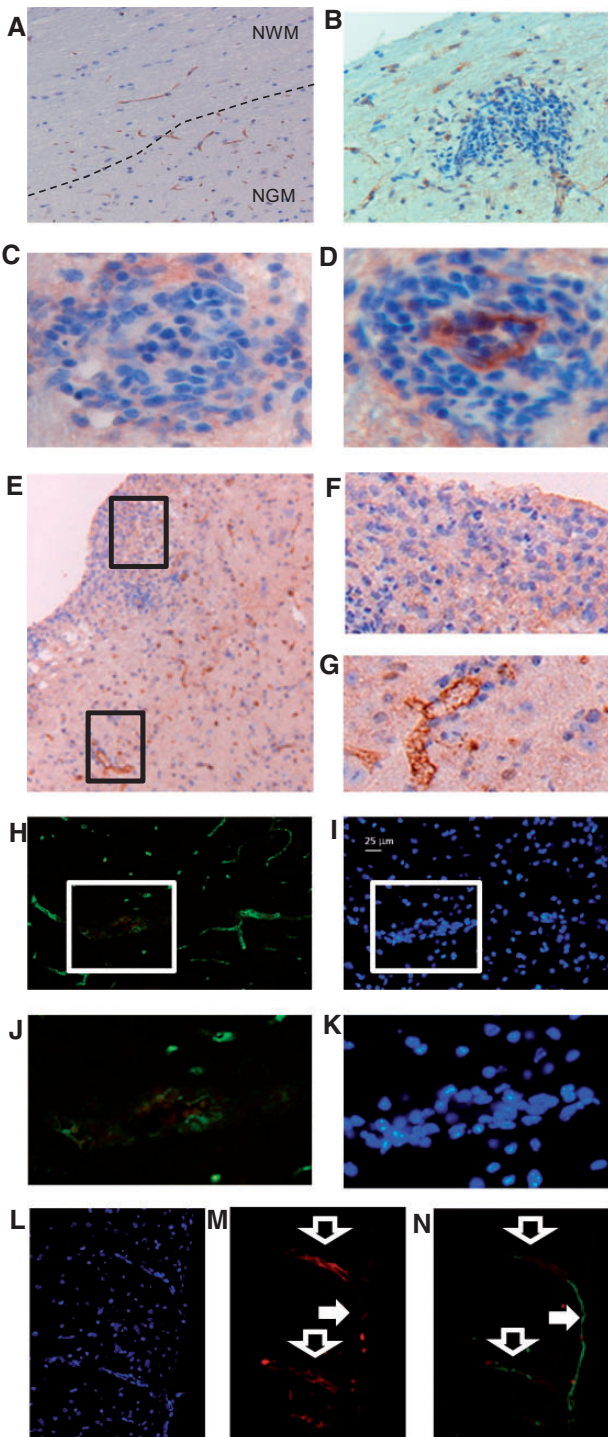
Figure 4 Selective loss of p-glycoprotein in EAE lesions. (**A**) Expression of p-glycoprotein in the spinal cord of normal animals detected by indirect immunoperoxidase staining. Dashed line indicates border of normal white matter (NWM) and normal grey matter (NGM). (**B**) Loss of vascular expression in an infiltrated perivascular lesion during relapse phase EAE. (**C**) Loss of vascular expression of p-glycoprotein in acute EAE lesion. (**D**) BCRP expression in a perivascular lesion in EAE. (**E–G**) Lesion in acute EAE. (**F**) High power of subpial lesion with loss of p-glycoprotein expression from **E**. (**G**) High power of non-inflamed blood vessel expressing p-glycoprotein from **E**. (**H–N**) Immunofluorescence

Therefore local delivery to injured neurons of p-glycoprotein substrates that are normally excluded from the CNS may allow selective targeting of drugs to EAE and multiple sclerosis lesions.

Production of a lesion-targeting central nervous system-excluded, sodium-channel blocking agent

A series of sodium channel blockers were synthesized (Clutterbuck et al., 2009), and to test our hypothesis, we generated a number of molecules, of which, CFM6104 [N-((5-(2-(2-(1h-imidazol-1-yl)ethyl)-2h-indazol-3-yl)-1,2,4-oxadiazol-3-yl)methyl)-3-methyl-benzamid] exhibited moderately favourable pharmacokinetic properties (Browne et al., submitted for publication). This molecule was predicted to be traceable using fluorescence because of the presence of an indazole group in the structure and had a blood/brain partition coefficient (Rishton et al., 2006) of −0.72 that would predict ∼80% CNS exclusion. Using membranes transfected with human ABCB1 (Fig. 6A) and a Caco-2 bioassay (Table 1) the compound was found to be a p-glycoprotein substrate and, accordingly, its transport was facilitated by the p-glycoprotein inhibitor cyclosporin A. These findings indicated that the transporter would normally actively remove CFM6104 from the CNS. When administered intravenously, CFM6104, failed to exhibit marked brain penetration at C_{max} indicative of CNS exclusion following intravenous administration (Table 2). The intraperitoneal route gave a better duration of action than the oral route and was used for in vivo studies. Following intraperitoneal injection of CFM6104 to ABH mice there was >90% exclusion in the spinal cord (Table 3). In EAE there was no apparent enhancement of CNS penetration, despite a significantly ($P < 0.001$) higher plasma level than in healthy animals (Table 3). This is probably related to a slowing of drug metabolism following the development of hypothermia that develops in the mice during periods of immobility during active EAE (Al-Izki et al., 2012). However, as CFM6104 was a naturally fluorescent compound, it could be traced. It was found to be excluded from the CNS in normal animals (Fig. 6B and C) but was able to access inflammatory lesions in the spinal cords of EAE animals (Fig. 6D and E). This indicated that the drug was indeed targeting and penetrating lesions,

Figure 4 Continued
staining demonstrating loss of p-glycoprotein. (**E**) Loss of p-glycoprotein expression in the perivascular lesion during EAE. Lesion in the white matter of spinal cord of mice stained to detect (**H**) p-glycoprotein or (**I**) DAPI. (**J and K**) Higher power of the EAE lesion depicted in **H** and **I**. The figure demonstrates selective loss of p-glycoprotein within lesions and demonstrates the lumen of the blood vessel indicated the presence of endothelia within the section. (**L–N**) Spinal cord from progressive EAE during remission from active paralysis. Although active inflammation may be less (**L**) DAPI staining, (**M**) endothelia detected through FITC-detected glucose transporter Glut-1 may (open arrow) or may not (filled arrow) co-express (**N**) p-glycoprotein-detected using rhodamine-labelled antibodies.
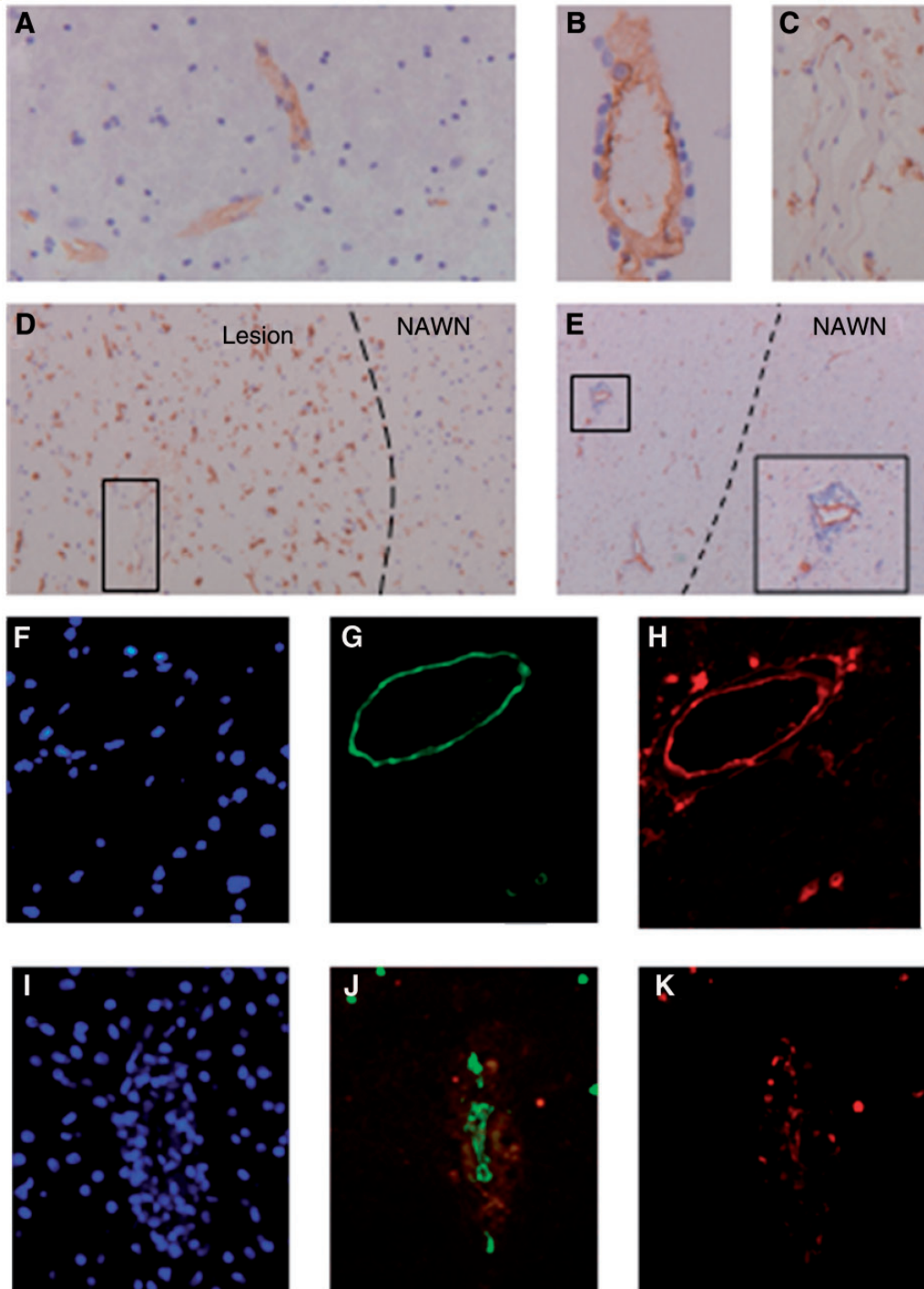
Figure 5 Selective loss of p-glycoprotein in multiple sclerosis lesions. (**A–E**) Indirect immunoperoxidase staining using diaminobenzidine substrate and haematoxylin counterstain of (**A**) control (heart attack) human brain, (**B–K**) multiple sclerosis brain, (**B**) blood vessel in normal appearing white matter (NAWM) and (**C**) chronic inactive multiple sclerosis lesion. (**D**) Low magnification of **D** showing chronic inactive lesion containing vessels that lack p-glycoprotein and astrocytes expressing p-glycoprotein and surrounding normal appearing white matter. (**E**) The expression of BCRP is maintained within lesions in a chronic active lesion and surrounding normal-appearing white matter. (**F–K**) Indirect immunofluorescence staining of p-glycoprotein in (**F–H**) normal appearing white matter and (**I–K**) active multiple sclerosis lesion. Sections were stained with (**F** and **I**) DAPI, (**G** and **J**) Glut-1 to detect endothelia (**H** and **K**) and rhodamine detected p-glycoprotein. (**G** and **H**) In normal appearing white matter endothelia clearly express p-glycoprotein. (**J** and **K**) In active lesions endothelia may downregulate p-glycoprotein.

Table 1 Compounds (1 μM) assayed for monolayer permeation using CacoReady™ assay

Drug	Efflux ratio (external versus internal)	
	Drug alone	Drug + CacoReady™ assay
Atenolol	0.3	Not done
Pindolol	1.3	Not done
Propanolol	0.8	Not done
Indinavir (+ control)	38.5	1.34
CFM6104	41.1	2.72

Caco2 cells were grown on a membrane; compounds were added to the apical or basolateral compartments and assayed in those compartments by LC-MS 2 h later. Drug concentrations were quantified by LC-MS/MS.

Table 2 Pharmacokinetics of CFM6104 assessed using LC-MS in mice injected with 5 mg/kg intravenous or 10 mg/kg intraperitoneal CFM6104

Time (min)	Mean CFM6104 levels (pg/μl)		
	Plasma (intraperitoneal)	Plasma (intravenous)	Brain (intravenous)
5	445 ± 71	1107 ± 32	$<3.0 \pm 0.0$
15	373 ± 38	212 ± 6	$<3.0 \pm 0.0$
30	129 ± 12	63 ± 24	$<3.0 \pm 0.0$

The results show the mean ($n = 3$) amount of compound detected.

Table 3 Normal ABH or paralysed ABH mice with EAE ($n = 3$–4) injected 30 min earlier with 10 mg/kg intraperitoneal CFM6104

Mice	Drug	n	Mean CFM6104 levels (pg/μl)	
			Plasma	Spinal cord
Normal	Vehicle	4	$<1.0 \pm 0.0$	$<1.0 \pm 0.0$
Normal	CFM6104	4	124.0 ± 34.2	10.0 ± 6.4
EAE	CFM6104	3	$985.0 \pm 90.4*$	18.9 ± 6.8

The results represent mean ± SEM levels. * P < 0.05 compared to normal mice.

presumably by a mechanism involving downregulation of p-glyco-protein at the blood–brain barrier in the vicinity of lesions.

Neuroprotective effect of a central nervous system-excluded, lesion targeting sodium-channel blocker

The dominant antigen in spinal cord-induced EAE in ABH mice is within the proteolipid protein that gives a poor *in vitro* proliferative response (Pryce *et al.*, 2005; Smith *et al.*, 2005). Therefore, the immunosuppressive effect of CFM6104 on T cell function was investigated using a simple contact-hypersensitivity paradigm that has been used to identify *in vivo* immunosuppressive doses (Watson *et al.*, 1991; Baker *et al.*, 1992; O'Neill *et al.*, 1992). Compared with vehicle treatment, CMF6104 failed to inhibit

lymph node proliferative responses after daily intraperitoneal administration of 5 mg/kg, 25 mg/kg and 50 mg/kg from a day before sensitization to the time of collecting the lymph nodes (Browne *et al.*, submitted for publication). Therefore, it was felt unnecessary to dose-titrate CFM6104 to avoid any immunosuppression-induced neuroprotection that could mask any real neuroprotective action of this drug. To limit animal usage required for a full-dose-response study, we selected 10 mg/kg CFM6104 administered intraperitoneally as a proof of principle dose. This dose was within the range used in humans for sodium channel-blocking agents (1–50 mg/kg *per os*), particularly when scaled to mouse and was well below the maximum tolerated dose (>50 mg/kg/daily). Intraperitoneal administration of 10 mg/kg CFM6104 was used to investigate its neuroprotective potential in an induced-relapse during EAE. The lack of immunosuppressive activity of CFM6104 was indicated further by the observation that CMF6104 did not significantly ($P > 0.05$) inhibit the incidence, onset, or maximum severity of relapsing EAE (Fig. 7A and B). Although CFM6104 did not inhibit the severity of paralysis during relapse (Fig. 7A), consistent with a lack of overt lymphoid cell immunosuppression, it did promote a significantly ($P < 0.01$) greater degree of recovery of motor-function during remission (Fig. 7B). This could be seen using the subjective clinical scoring system (Fig. 7B) and objective motor-function using the RotaRod ($P < 0.001$, Fig. 7C). These improved motor outcomes were paralleled by the ability of CMF6104 to reduce spinal cord nerve loss, a consequence of relapsing disease, as assessed by an ELISA specific for neurofilament, (Fig. 7D). Therefore, CMF6104 did exhibit a neuroprotective effect and slowed the loss of nerves due to inflammatory attack.

Discussion

This study provides further evidence that Na$_v$ blockers have the potential to limit nerve loss in the progressive phase of EAE. Although this finding is not novel, this current study differs from many in that the clinical activity is not simply secondary to an immunosuppressive action exerted within the CNS (Lo *et al.*, 2003; Black *et al.*, 2007). In the present study the compounds were delivered to sensitized animals with disease at a time that does not to interfere with priming of T cells and at a dose with no overt T cell immunosuppression; based on the clinical profile and *ex vivo* T cell assays as shown with carbamazepine, oxcarbamazepine and CFM6104. Interestingly, inhibition of T cell responses was not seen either with boluses of 1, 10 and 30 mg/kg phenytoin (50 mg/kg was toxic) (unpublished observation) or in the rat with lamotrigine (Bechtold *et al.*, 2006) and contrasts with that seen with peripherally-active immunosuppressive agents (Baker *et al.*, 1992; O'Neill *et al.*, 1993). Although we have not seen immunosuppressive activity in the Na$_v$ blockers we examined, such an activity could be of additional benefit in arresting autoimmune-dependent neurodegeneration. It has been shown that prophylactic peripheral immunosuppression can account for the protection of EAE (Black *et al.*, 2007), however, therapeutic doses of agents used here were not overtly T cell immunosuppressive. The degree of inflammation was not directly measured in the EAE as clinical
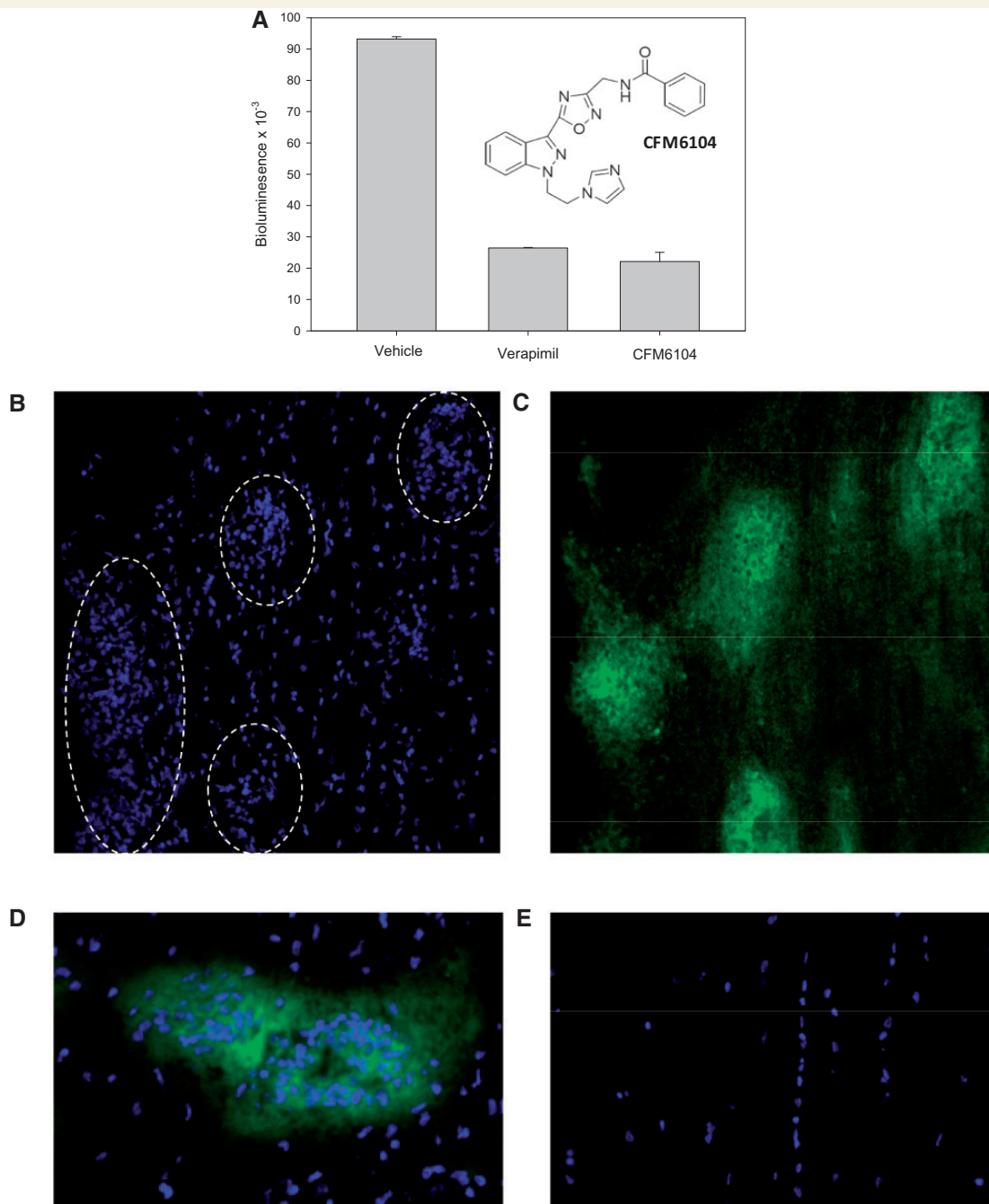
Figure 6 CMF6104 is a CNS-excluded, p-glycoprotein substrate that penetrates EAE lesions. (**A**) Vehicle, verapamil (100 μM) and CFM6104 (100 μM) were tested as substrates for p-glycoprotein assessed in the Pgp-Glow assay. The results represent the mean ± SEM (triplicates) bioluminescence measurements from the luciferin reporter. The inset shows the structure of CFM6104. (**B–E**) Cryostat sections of spinals cords from animals injected 30 min earlier with 20 mg/kg intraperitoneal CFM6104 and perfused with PBS before collection of spinal cords (**E–G**) paralysed (grade 4 and losing weight) EAE mice or (**E**) a normal mouse. (**B**) EAE section stained with DAPI (blue) demonstrating lesions (white dashed line), (**C**) extravasation of CFM6104 (green) in the same lesions or (**D** and **E**) double staining for DAPI and CFM6104.

course was the primary outcome measure; however, the degree of inflammation directly correlates with the severity of clinical disease during disease development and is dynamic such that inflammatory infiltrates are lost as animals begin to remit (Baker *et al.*, 1990, 2011; Allen *et al.*, 1993; Wujek *et al.*, 2002; Jackson *et al.*, 2009). In this study there was no indication of immunosuppression of the generation of inflammation as assessed histologically in the uveitis model and by the fact that the onset and
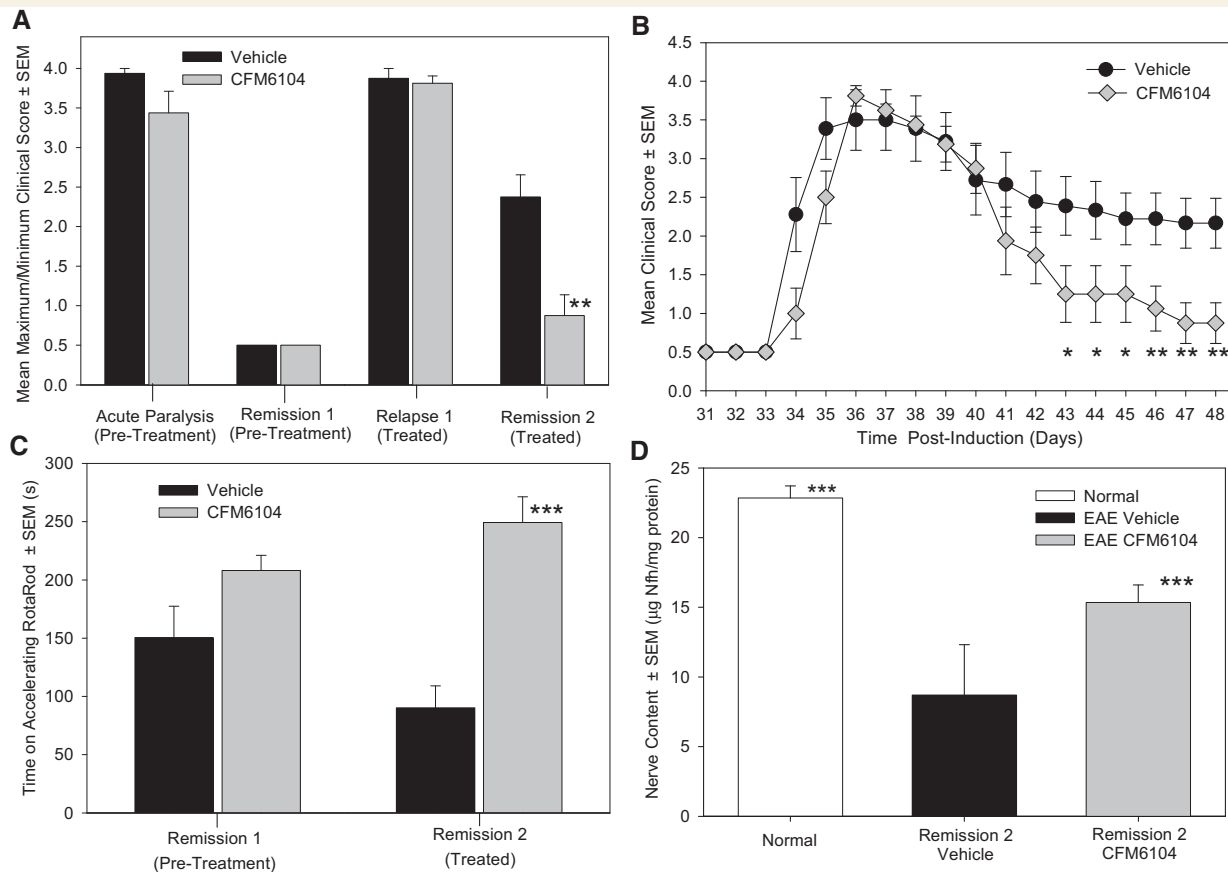
Figure 7 CFM6104 inhibits the accumulation of neurological deficit and neurodegeneration during EAE. ABH mice were injected with 1 mg mouse spinal cord homogenate in Freund's adjuvant on Days 0 and 7 post induction to induce EAE and this was repeated on Day 27 post induction to induce a relapse. Animals were injected intraperitoneally daily with either vehicle or 10 mg/kg CFM6104 from Day 33 onwards. Animals were monitored for the development of clinical disease and the results represent: (**A**) the mean maximal clinical score, during the initial acute attack ∼Days 15–20 and the clinical relapse ∼Days 34–40, or the mean minimal clinical score during remission from paralytic attacks. (**B**) The mean daily clinical score following induction of relapse. (**C**) The time taken to fall from an accelerating RotaRod was monitored pre-treatment on Day 25 or on Day 48 post-disease induction, when the experiment was terminated. (**D**) The spinal cords were removed and nerve content was measured using a neurofilament heavy chain (Nfh)-specific ELISA. The results represent the mean ± SEM of eight animals per group. *$P < 0.05$, **$P < 0.01$, ***$P < 0.001$ compared with vehicle-treated animals.

severity of clinical disease was unaffected. However, inhibition of peripheral immunity preventing lesion formation (Black *et al.*, 2007) in addition to anti-inflammatory effects within the CNS once lesions form (Bechtold *et al.*, 2006; Morsali *et al.*, 2013) and direct neuroprotection by an action on nerves (Fern *et al.*, 1993; Garthwaite *et al.*, 1999; Kapoor *et al.*, 2003) will contribute to the overall neuroprotective potential of this class of agents.

Clinical trials in multiple sclerosis of sodium channel blockers have been halted because of concern about a rebound effect following cessation of treatment that occurred in animals (Black *et al.*, 2007; Waxman, 2008). This can occur when immunosuppressive doses of compounds that prevent disease development are removed, which allows CNS autoimmunity to return (Greenwood *et al.*, 2003; Black *et al.*, 2007). As the compounds reported here were found not to be immunosuppressive and did not inhibit the generation of relapse, we would not anticipate, and did not look for, a rebound effect following cessation of treatment. However, in the absence of peripheral immunosuppression, sodium channel blockade also induces a neuroprotective anti-

inflammatory effect through inhibition of microglial function (Bechtold *et al.*, 2006; Morsali *et al.*, 2013). Lamotrigine treatment resulted in what was thought to be pseudoatrophy in brain volume because of some anti-inflammatory effect reducing tissue oedema (Kapoor *et al.*, 2010). Following cessation of lamotrigine treatment brain volume increased suggestive of some return of disease activity, but this was not associated with a rebound exacerbation in secondary progressive multiple sclerosis (Kapoor *et al.*, 2010).

We have previously demonstrated that the neurofilament ELISA provides a good correlate to histological assessment of axon numbers (Jackson *et al.*, 2005, 2009; Al-Izki *et al.*, 2012) and neurofilament release into biological fluids as a consequence of nerve damage is a reliable biomarker for neurodegeneration in people with multiple sclerosis and other disorders (Gunnarsson *et al.*, 2011; Gnanapavan *et al.*, 2013). Neurofilament measurement offers the advantage of rapid analysis of the whole spinal cord and provides an outcome measure that can be translated into human disease (Gunnarsson *et al.*, 2011; Gnanapavan *et al.*,

2012, 2013). This technique lacks the bias associated with the use of histological analysis, which is not only time-consuming but invariably focuses analysis on restricted-CNS tracts. Any marked neuroprotection by Na$_v$ blockers in sensory tracts may not be reflected in the motor outcomes measures (Lo et al., 2003; Bechtold et al., 2006). Clinical scoring systems commonly used in EAE have been developed to assess active paralysis similar to the Expanded Disability Status Scale (EDSS) that is used for multiple sclerosis. These are subjective, user-dependent and are subject to bias of analysis, as treatment effects are greater in studies not reporting blinding (Vesterinen et al., 2010). Furthermore, they are non-linear scales that are insensitive to change. This is especially the case in assessing functional deficits in animals that occur as a consequence of paralytic attacks (Al-Izki et al., 2012). However, residual neurological deficit after attack can be used to detect neuroprotective effects (Baker et al., 2011). More importantly the accelerating RotaRod appears to be a sensitive, objective and quantitative outcome measure that can detect motor deficits and functional improvements during remission from paralytic attacks (Al-Izki et al., 2011, 2012). This shows a strong correlation with spinal nerve content (Al-Izki et al., 2012). These two outcomes together showed significant treatment responsiveness to Na$_v$ blockade. In addition, the use of the novel optic neuritis model provides a further tool to confirm the neuroprotective effects of sodium channel blockers.

Although it has been reported that the Na$_v$ blocker lamotrigine is ineffective in progressive multiple sclerosis (Kapoor et al., 2010), it is premature to discard this class of agents on the basis of this result. Lamotrigine did not appear to influence the course of multiple sclerosis, except perhaps by slowing the decline in the 25 m walk (Kapoor et al., 2010). However, lamotrigine in comparison with other compounds is a weak neuroprotectant in vitro (Garthwaite et al., 1999). In preclinical EAE studies (group sizes of n = 70), lamotrigine demonstrated a marginal (P < 0.05) clinical improvement and histological analysis of selected sensory nerve tracts showed a 30% reduction in axonal loss in a subset (50% of animals) of the experimental animals (Bechtold et al., 2006). Moreover, in a trial in patients with multiple sclerosis, the primary MRI outcome measure of cerebral volume was complicated by accelerated atrophy in the first year as mentioned previously. Unfortunately, the trial was too short to accommodate pseudoatrophy in a positive fashion (Kapoor et al., 2010). Furthermore, the patient cohort may not have been optimal for this study. The disease in the placebo group was slowly progressing with few clinical changes from baseline. Importantly, the drug was also poorly tolerated (Kapoor et al., 2010). This was indicated by the high number of drop-outs during the study, the inability of many to reach the target anti-epileptic dose because of side effects and most importantly, the observation that ~40–50% of patients in the active arm were not drug-compliant as defined by serum levels (Kapoor et al., 2010; Gnanapavan et al., 2013; Raftopoulos and Kapoor, 2013). Therefore, it is not surprising that the main study failed to show a drug effect. Nevertheless, there was a significant reduction in serum neurofilament levels between placebo and drug-compliant individuals, indicating that Na$_v$ blockage was neuroprotective (Gnanapavan et al., 2013), as found here in EAE. Therefore, study of people with multiple sclerosis at earlier stages of their disease, when they can better tolerate Na$_v$ blockage is warranted.

We demonstrate that Na$_v$ blockade is neuroprotective in a novel experimental optic neuritis model that exhibits subclinical EAE and offers a less severe, 3Rs-refined alternative to classical paralytic EAE. Both oxcarbazepine and carbamazepine inhibited the consequences of optic neuritis in the optic nerve that is reflected by loss of retinal ganglion cells in the retina (Bettelli et al., 2003; Guan et al., 2006). This is consistent with the neuroprotective effect of 5 mg/kg intraperitoneal of CFM6104 in the same model and treatment paradigm that produced significant (P < 0.05) neuroprotection of retinal ganglion cells (Browne et al., submitted for publication). This concept is currently being tested in an optic neuritis trial (Raftopoulos and Kapoor, 2013).

Although a desired mechanism for treatment of progressive multiple sclerosis is through prevention of sodium loading in nerves (Dutta and Trapp, 2011), the neuroprotective influence found here is probably anti-inflammatory within the CNS. While the data may suggest that such sodium channel blockade may have some benefit in the control of progression, the results of the current study are best translated to treatment during relapsing multiple sclerosis. Further studies to examine the influence in post-relapsing secondary progressive EAE (Al-Izki et al., 2011) are warranted to explore the neuroprotective potential of sodium channel blockade for progressive multiple sclerosis. That p-glycoprotein is lost in chronic inactive lesions, where blood–brain barrier dysfunction is reduced, may allow neuroprotection of demyelinated nerves to be targeted. These are particularly vulnerable to damage due to metabolic demands required to maintain conduction following rearrangement of Na$_v$1.6 from the nodes of Ranvier during demyelination (Craner et al., 2004). Low levels of these receptors are expressed along the length of demyelinated axons and the novel expression of Na$_v$1.2 occurs on these nerves to maintain conduction (Craner et al., 2004). Local targeting of axonal conduction in areas of myelin-denuded axon may, however, still cause some negative symptomatic deficits because of impedance mismatch and through influences of low density of sodium channels on demyelinated axons (Waxman and Brill, 1978). Although the risk of this is perhaps reduced compared to the globally active fully penetrant CNS compounds, side effects were not noticed during this study; however, the aim was not to induce toxicity and therefore low doses of compounds were used. Nevertheless, it was noted that although doses of 50 mg/kg intraperitoneal CFM6104 were well tolerated, phenytoin induced toxicity and caused fatality at the same dose, supporting the concept that CNS-excluded compounds may have a better tolerability profile.

It is known that Na$_v$ blockers inhibit macrophage and microglial activation (Black and Waxman, 2012; Morsali et al., 2013). Through this mechanism, the neurodegenerative effect of the inflammatory-penumbra that is formed around the perivascular lesions by T cell invasion correlates in time with the period of active blood–brain barrier dysfunction. In mice, this 'inflammatory penumbra' lasts for a few days and correlates with the period of time that the blood–brain barrier is disrupted. In humans, it is likely to be longer because acute inflammatory multiple sclerosis lesions are known to enhance with gadolinium on MRI, signifying blood–brain barrier dysfunction for a few weeks (Butter et al.,

1991; Cotton et al., 2003; Al-Izki et al., 2012). For this reason we are recruiting and dosing volunteers for the acute optic neuritis study (NCT01451593; Raftopoulos and Kapoor, 2013) within 14 days of disease onset, when lesions would have focal disruption of the blood–brain barrier as detected with gadolinium-enhanced MRI. Furthermore, as there are many more MRI lesions than clinical attacks the approach of selectively targeting lesions is important even when the disease is in apparent clinical remission. Although our studies may indicate an anti-inflammatory effect, which may occur in multiple sclerosis as seen by a reduction in tissue oedema (Kapoor et al., 2010), this is unlikely to be because of a lymphoid cell immunosuppressive effect that is hypothesized to drive relapsing disease. Therefore, an optimal therapeutic strategy may require a combination of a systemic immunosuppressive agent combined with a neuroprotective agent. We initially examined carbamazepine, which has side effects such as drowsiness, dizziness, ataxia and nausea in humans. However, oxcarbazepine, which is an analogue of carbamazepine, was slightly more active as a neuroprotectant in our hands and has a lower incidence of side effects and is therefore better tolerated (Elger and Bauer, 1998). We therefore plan to use oxcarbazepine in another novel trial (Protective Role of OXcarbazepine In MUltiple Sclerosis or PROXIMUS study) that will use neurofilament levels in serial CSF analyses as the primary outcome measure. This provides another example of how animal studies can help inform the development of new treatments for people with multiple sclerosis.

Loss of p-glycoprotein expression in multiple sclerosis has been independently confirmed and it has been shown that p-glycoprotein is lost in active, chronic active and chronic inactive multiple sclerosis lesions (Kooij et al., 2010, 2011). Blockade of p-glycoprotein enhances brain penetration of p-glycoprotein substrates as shown using PET (Nojiri et al., 2008) and therefore loss of vascular p-glycoprotein may potentially allow targeting of acute multiple sclerosis lesions similarly to the way in which active EAE lesions were targeted here. Despite this potential benefit for pharmacotherapy, loss of p-glycoprotein expression may contribute to the neurotoxicity that drives progression of the disease. Downregulation of p-glycoprotein occurs after CD54 cross-linking associated with leucocyte diapedesis (Kooij et al., 2010). However, there are other factors that regulate p-glycoprotein expression (Miller et al., 2008) and loss of p-glycoprotein is observed in both chronic active and importantly chronic inactive lesions, which are not all associated with perivascular cuffing as shown here. Therefore, Na$_v$ blocking agents that are p-glycoprotein substrates would be able to inhibit both the progressive neurodegenerative processes in nerves and the glial cell activation that drive neurodegeneration in vivo. We have produced a Na$_v$ blocker that was selectively CNS-excluded and traceable. However, LC-MS studies failed to demonstrate CFM6104 penetration during EAE, which was surprising because active disease is associated with blood–brain barrier dysfunction in the spinal cord (Al-Izki et al., 2012). This suggests that either only small amounts were penetrating the lesions or that CNS CFM6104 was not being detected because of technical reasons such as binding of the hydrophobic compound to CNS structures, (e.g. myelin) or it was rapidly metabolized in the brain. However, the compound could be seen to penetrate the lesions and this had an action consistent with CNS

penetration and may indicate that only small amounts of compound are required for a biological effect.

Current Na$_v$ blockers, given their general hydrophobicity, may be expected to show some affinity for ABC efflux transporters and thus may partially exploit this targeting approach (Crowe and Teoh, 2006; Nakanishi et al., 2013). CFM6104 is a CNS-excluded p-glycoprotein substrate and yet it clearly targeted lesions during EAE and induced neuroprotection. Although CFM6104 was sufficient to provide proof of principle, further development of this class of compound is warranted to improve potency at the target and predicted pharmacokinetic profile. This selective targeting strategy could be developed for other drugs, where global CNS penetration and receptor stimulation may be problematic, and provides new avenues for future treatment of multiple sclerosis.

Acknowledgements

Funding

Conflict of interest

D.B., L.C., J.G., C.P. and D.L.S. have filed patents related to the compounds used in this study. G.G. has provided consultancies for many pharmaceutical companies in the multiple sclerosis field. This had no influence on the design and execution of this study.

References

Al-Izki S, Pryce G, O'Neill JK, Butter C, Giovannoni G, Amor S, et al. Practical guide to the induction of relapsing progressive experimental autoimmune encephalomyelitis in the Biozzi ABH mouse. Mult Scler Relat Dis 2012; 1: 29–38.

Al-Izki S, Pryce G, Jackson SJ, Giovannoni G, Baker D. Immunosuppression with FTY720 is insufficient to prevent secondary progressive neurodegeneration in experimental autoimmune encephalomyelitis. Mult Scler 2011; 17: 939–48.

Allen SJ, Baker D, O'Neill JK, Davison AN, Turk JL. Isolation and characterization of cells infiltrating the spinal cord during the course of chronic relapsing experimental allergic encephalomyelitis in the Biozzi AB/H mouse. Cell Immunol 1993; 146: 335–50.

Amor S, Groome N, Linington C, Morris MM, Dornmair K, Gardinier MV, et al. Identification of epitopes of myelin oligodendrocyte glycoprotein for the induction of experimental allergic encephalomyelitis in SJL and Biozzi AB/H mice. J Immunol 1994; 153: 4349–56.

Baker D, Gerritsen W, Rundle J, Amor S. Critical appraisal of animal models of multiple sclerosis. Mult Scler 2011; 17: 647–57.

Baker D, O'Neill JK, Davison AN, Turk JL. Control of immune-mediated disease of the central nervous system requires the use of a neuroactive agent: elucidation by the action of mitoxantrone. Clin Exp Immunol 1992; 90: 124–8.

Baker D, O'Neill JK, Gschmeissner SE, Wilcox CE, Butter C, Turk JL. Induction of chronic relapsing experimental allergic encephalomyelitis in Biozzi mice. J Neuroimmunol 1990; 28: 261–70.

Bechtold DA, Miller SJ, Dawson AC, Sun Y, Kapoor R, Berry D, et al. Axonal protection achieved in a model of multiple sclerosis using lamotrigine. J Neurol 2006; 253: 1542–51.

Bettelli E, Pagany M, Weiner HL, Linington C, Sobel RA, Kuchroo VK. Myelin oligodendrocyte glycoprotein-specific T cell receptor transgenic mice develop spontaneous autoimmune optic neuritis. J Exp Med 2003; 197: 1073–81.

Black JA, Liu S, Carrithers M, Carrithers LM, Waxman SG. Exacerbation of experimental autoimmune encephalomyelitis after withdrawal of phenytoin and carbamazepine. Ann Neurol 2007; 62: 21–33.

Black JA, Liu S, Hains BC, Saab CY, Waxman SG. Long-term protection of central axons with phenytoin in monophasic and chronic-relapsing EAE. Brain 2006; 129 (Pt 12): 3196–208.

Black JA, Waxman SG. Sodium channels and microglial function. Exp Neurol 2012; 234: 302–15.

Butter C, Baker D, O'Neill JK, Turk JL. Mononuclear cell trafficking and plasma protein extravasation into the CNS during chronic relapsing experimental allergic encephalomyelitis in Biozzi AB/H mice. J Neurol Sci 1991; 104: 9–12.

Clutterbuck LA, Posada CG, Visintin C, Riddall DR, Lancaster B, Gane PJ, et al. Oxadiazolylindazole sodium channel modulators are neuroprotective toward hippocampal neurones. J Med Chem 2009; 52: 2694–707.

Coles AJ, Wing MG, Molyneux P, Paolillo A, Davie CM, Hale G, et al. Monoclonal antibody treatment exposes three mechanisms underlying the clinical course of multiple sclerosis. Ann Neurol 1999; 46: 296–304.

Compston A, Coles A. Multiple sclerosis. Lancet 2008; 372: 1502–17.

Cotton F, Weiner HL, Jolesz FA, Guttmann CR. MRI contrast uptake in new lesions in relapsing-remitting MS followed at weekly intervals. Neurology 2003; 60: 640–6.

Craner MJ, Damarjian TG, Liu S, Hains BC, Lo AC, Black JA, et al. Sodium channels contribute to microglia/macrophage activation and function in EAE and MS. Glia 2005; 49: 220–9.

Craner MJ, Newcombe J, Black JA, Hartle C, Cuzner ML, Waxman SG. Molecular changes in neurons in multiple sclerosis: altered axonal expression of Nav1.2 and Nav1.6 sodium channels and Na + /Ca2 + exchanger. Proc Natl Acad Sci USA 2004; 101: 8168–73.

Crowe A, Teoh YK. Limited P-glycoprotein mediated efflux for anti-epileptic drugs. J Drug Target 2006; 14: 291–300.

Dutta R, Trapp BD. Mechanisms of neuronal dysfunction and degeneration in multiple sclerosis. Prog Neurobiol 2011; 93: 1–12.

Elger CE, Bauer J. New antiepileptic drugs in epileptology. Neuropsychobiology 1998; 38: 145–8.

Feng G, Mellor RH, Bernstein M, Keller-Peck C, Nguyen QT, Wallace M, et al. Imaging neuronal subsets in transgenic mice expressing multiple spectral variants of GFP. Neuron 2000; 28: 41–51.

Fern R, Ransom BR, Stys PK, Waxman SG. Pharmacological protection of CNS white matter during anoxia: actions of phenytoin, carbamazepine and diazepam. J Pharmacol Exp Ther 1993; 266: 1549–55.

Garthwaite G, Brown G, Batchelor AM, Goodwin DA, Garthwaite J. Mechanisms of ischaemic damage to central white matter axons: a quantitative histological analysis using rat optic nerve. Neuroscience 1999; 94: 1219–30.

Gnanapavan S, Grant D, Morant S, Furby J, Hayton T, Teunissen CE, et al. Biomarker Report from the Phase II Lamotrigine Trial in Secondary Progressive MS - Neurofilament as a Surrogate of Disease Progression. PLoS One 2013; 8: e70019.

Gnanapavan S, Grant D, Pryce G, Jackson S, Baker D, Giovannoni G. Neurofilament a biomarker of neurodegeneration in autoimmune encephalomyelitis. Autoimmunity 2012; 45: 298–303.

Greenwood J, Walters CE, Pryce G, Kanuga N, Beraud E, Baker D, et al. Lovastatin inhibits brain endothelial cell Rho-mediated lymphocyte migration and attenuates experimental autoimmune encephalomyelitis. FASEB J 2003; 17: 905–7.

Guan Y, Shindler KS, Tabuena P, Rostami AM. Retinal ganglion cell damage induced by spontaneous autoimmune optic neuritis in MOG-specific TCR transgenic mice. J Neuroimmunol 2006; 178: 40–8.

Gunnarsson M, Malmestrom C, Axelsson M, Sundstrom P, Dahle C, Vrethem M, et al. Axonal damage in relapsing multiple sclerosis is markedly reduced by natalizumab. Ann Neurol 2011; 69: 83–9.

Hampton DW, Anderson J, Pryce G, Irvine KA, Giovannoni G, Fawcett JW, et al. An experimental model of secondary progressive multiple sclerosis that shows regional variation in gliosis, remyelination, axonal and neuronal loss. J Neuroimmunol 2008; 201–02; 200–11.

Hankey DJ, Lightman SL, Baker D. Interphotoreceptor retinoid binding protein peptide-induced uveitis in B10.RIII mice: characterization of disease parameters and immunomodulation. Exp Eye Res 2001; 72: 341–50.

Jackson SJ, Lee J, Nikodemova M, Fabry Z, Duncan ID. Quantification of myelin and axon pathology during relapsing progressive experimental autoimmune encephalomyelitis in the Biozzi ABH mouse. J Neuropathol Exp Neurol 2009; 68: 616–25.

Jackson SJ, Pryce G, Diemel LT, Cuzner ML, Baker D. Cannabinoid-receptor 1 null mice are susceptible to neurofilament damage and caspase 3 activation. Neuroscience 2005; 134: 261–8.

Kapoor R, Davies M, Blaker PA, Hall SM, Smith KJ. Blockers of sodium and calcium entry protect axons from nitric oxide-mediated degeneration. Ann Neurol 2003; 53: 174–80.

Kapoor R, Furby J, Hayton T, Smith KJ, Altmann DR, Brenner R, et al. Lamotrigine for neuroprotection in secondary progressive multiple sclerosis: a randomised, double-blind, placebo-controlled, parallel-group trial. Lancet Neurol 2010; 9: 681–8.

Kooij G, Mizee MR, van Horssen J, Reijerkerk A, Witte ME, Drexhage JA, et al. Adenosine triphosphate-binding cassette transporters mediate chemokine (C-C motif) ligand 2 secretion from reactive astrocytes: relevance to multiple sclerosis pathogenesis. Brain 2011; 134 (Pt 2): 555–70.

Kooij G, van Horssen J, de Lange EC, Reijerkerk A, van der Pol SM, van Het Hof B, et al. T lymphocytes impair P-glycoprotein function during neuroinflammation. J Autoimmun 2010; 34: 416–25.

Lassmann H. Pathology and disease mechanisms in different stages of multiple sclerosis. J Neurol Sci 2013; 333: 1–4.

Lee Y, Morrison BM, Li Y, Lengacher S, Farah MH, Hoffman PN, et al. Oligodendroglia metabolically support axons and contribute to neurodegeneration. Nature 2012; 487: 443–8.

Lidster K, Jackson SJ, Ahmed Z, Munro P, Coffey P, Giovannoni G, et al. Neuroprotection in a novel mouse model of multiple sclerosis. PLoS One 2013; 8: e79188.

Lo AC, Saab CY, Black JA, Waxman SG. Phenytoin protects spinal cord axons and preserves axonal conduction and neurological function in a model of neuroinflammation *in vivo*. J Neurophysiol 2003; 90: 3566–71.

Marta M, Giovannoni G. Disease modifying drugs in multiple sclerosis: mechanisms of action and new drugs in the horizon. CNS Neurol Disord Drug Targets 2012; 11: 610–23.

Miller DS, Bauer B, Hartz AM. Modulation of P-glycoprotein at the blood-brain barrier: opportunities to improve central nervous system pharmacotherapy. Pharmacol Rev 2008; 60: 196–209.

Morsali D, Bechtold D, Lee W, Chauhdry S, Palchaudhuri U, Hassoon P, et al. Safinamide and flecainide protect axons and reduce microglial activation in models of multiple sclerosis. Brain 2013; 136 (Pt 4): 1067–82.

Nakanishi H, Yonezawa A, Matsubara K, Yano I. Impact of P-glycoprotein and breast cancer resistance protein on the brain distribution of antiepileptic drugs in knockout mouse models. Eur J Pharmacol 2013; 710: 20–8.

Nojiri Y, Ishiwata K, Qinggeletu , Tobiishi S, Sasada T, Yamamoto F, et al. Radiosynthesis and biodistribution in mice of a 18F-labeled analog of O-1302 for use in cerebral CB1 cannabinoid receptor imaging. Biol Pharm Bull 2008; 31: 1274–8.

O'Neill JK, Baker D, Davison AN, Allen SJ, Butter C, Waldmann H, et al. Control of immune-mediated disease of the central nervous system with monoclonal (CD4-specific) antibodies. J Neuroimmunol 1993; 45: 1–14.

O'Neill JK, Baker D, Davison AN, Maggon KK, Jaffee BD, Turk JL. Therapy of chronic relapsing experimental allergic encephalomyelitis and the role of the blood-brain barrier: elucidation by the action of Brequinar sodium. J Neuroimmunol 1992; 38: 53–62.

Parpura V, Verkhratsky A. Homeostatic function of astrocytes: Ca(2+) and Na(+) signalling. Transl Neurosci 2012; 3: 334–44.

Piddlesden SJ, Lassmann H, Zimprich F, Morgan BP, Linington C. The demyelinating potential of antibodies to myelin oligodendrocyte glycoprotein is related to their ability to fix complement. Am J Pathol 1993; 143: 555–64.

Pryce G, O'Neill JK, Croxford JL, Amor S, Hankey DJ, East E, et al. Autoimmune tolerance eliminates relapses but fails to halt progression in a model of multiple sclerosis. J Neuroimmunol 2005; 165: 41–52.

Raftopoulos RE, Kapoor R. Neuroprotection for acute optic neuritis-can it work? Mult Scler Rel Dis 2013; 2: 307–11.

Rishton GM, LaBonte K, Williams AJ, Kassam K, Kolovanov E. Computational approaches to the prediction of blood-brain barrier permeability: a comparative analysis of central nervous system drugs versus secretase inhibitors for Alzheimer's disease. Curr Opin Drug Discov Devel 2006; 9: 303–13.

Smith PA, Morris-Downes M, Heijmans N, Pryce G, Arter E, O'Neill JK, et al. Epitope spread is not critical for the relapse and progression of MOG 8-21 induced EAE in Biozzi ABH mice. J Neuroimmunol 2005; 164: 76–84.

Vesterinen HM, Sena ES, ffrench-Constant C, Williams A, Chandran S, Macleod MR. Improving the translational hit of experimental treatments in multiple sclerosis. Mult Scler 2010; 16: 1044–55.

Watson CM, Davison AN, Baker D, O'Neill JK, Turk JL. Suppression of demyelination by mitoxantrone. Int J Immunopharmacol 1991; 13: 923–30.

Waxman SG. Mechanisms of disease: sodium channels and neuroprotection in multiple sclerosis-current status. Nat Clin Pract Neurol 2008; 4: 159–69.

Waxman SG, Brill MH. Conduction through demyelinated plaques in multiple sclerosis: computer simulations of facilitation by short internodes. J Neurol Neurosurg Psychiatry 1978; 41: 408–16.

Wujek JR, Bjartmar C, Richer E, Ransohoff RM, Yu M, Tuohy VK, et al. Axon loss in the spinal cord determines permanent neurological disability in an animal model of multiple sclerosis. J Neuropathol Exp Neurol 2002; 61: 23–32.